General Disclaimer

One or more of the Following Statements may affect this Document

- This document has been reproduced from the best copy furnished by the organizational source. It is being released in the interest of making available as much information as possible.

- This document may contain data, which exceeds the sheet parameters. It was furnished in this condition by the organizational source and is the best copy available.

- This document may contain tone-on-tone or color graphs, charts and/or pictures, which have been reproduced in black and white.

- This document is paginated as submitted by the original source.

- Portions of this document are not fully legible due to the historical nature of some of the material. However, it is the best reproduction available from the original submission.

PROGRESS REPORT

Analysis of Jovian Decametric Data:
Study of Radio Emission Mechanisms

covering the period
September 15, 1984 - March 15, 1985

submitted by

David H. Staelin
Tomas A. Arias

August 6, 1985

Massachusetts Institute of Technology
Research Laboratory of Electronics
Cambridge, Massachusetts 02139

I. Introduction

Data gathered by the Voyager 1 and Voyager 2 Planetary Radio Astronomy Experiments (PRA) are unique in many ways including their frequency range, time resolution, polarization information and geometric characteristics. The PRA instruments scan their frequency range, which consists of a 70-channel 1.2 KHz-1.3 MHz low-frequency (LF) band and a 128-channel 1.3 MHz-40.5 MHz high-frequency (HF) band, once every 6 seconds, alternately observing RHC or LHC polarized radiation with each step in frequency and with each scan. Studies of rapidly varying phenomena have thus far been hampered by paper display techniques which require large amounts of paper to exploit the full PRA time resolution and which are not sufficiently flexible to handle temporal and channel-to-channel variations in baseline, receiver sensitivity, signal strength and level of spacecraft interference. In September 1984, however, our group completed the development of a software package capable of effectively displaying full 6s resolution PRA dynamic spectra on our high quality video monitor while compensating for the aforementioned variations. We subsequently began the systematic conversion of PRA data to video images and have to date processed 193.52 hours of the Voyager 1 PRA data gathered within ~2 weeks of encounter.

We have called the most striking phenomena revealed by the new display techniques Modulated Spectral Activity (MSA) because of its appearance in dynamic spectra as a series of at least two parallel emission bands which drift back and forth in frequency on time scales of tens of seconds while approximately maintaining the differences in frequency among themselves (see Figure 1a). Though highly variable,

MSA emission bands nearly always occur within well-defined regions of the time-frequency plane. These regions, or storms, persist for periods of ~10 minutes and, though they usually develop on time scales of minutes, may start or stop within periods as small as a few scans (see Figure 1d). MSA emission bands have widths and spacings that vary from near or below the LF PRA frequency resolution of 19.2 KHz to maximums of ~120 and ~240 KHz, respectively (as in Figure 1c). MSA events have been observed at all frequencies from ~200 KHz to 1.3 MHz above which the (HF) PRA frequency resolution is insufficient to allow the unique identification of MSA. Nonetheless, LF MSA events which drift to 1.3 MHz are often contiguous with narrow banded HF features, suggesting that MSA does occur at frequencies above 1.3 MHz. We note that cyclotron frequencies in the range 200 KHz-1.3 MHz occur somewhat less than halfway out along L=6 field lines, a likely MSA source location in lieu of results presented in the next section. Finally, MSA dynamic spectra occasionally vary in appearance, sometimes appearing "washed out" as in Figure 1e or, perhaps due to aliasing caused by rapid drifting in frequency, taking on the appearance of an organized storm of S-bursts (as in Figure 1f or the HF MSA-like activity observed near encounter in Figure 1b), or even failing to occur within well-defined time-frequency ranges (Figure 1g).

II. Statistical Properties of MSA

In an attempt to locate and understand the MSA source mechanism, a catalogue has been compiled of the start and end of all known MSA events. This catalogue indicates pre-, near- (within 2 days), and post- encounter MSA occurrence probabilities (total MSA time divided by observation time) of 14.6±1.4%, ~0.8% and 9.7±3.3%, respectively.

(b)

FREQUENCY (MHZ)

0

1.3

40.5

0   12   24

RELATIVE TIME (MINUTES)

(a)

FREQUENCY (MHZ)

0

1.3

40.5

0   12   24
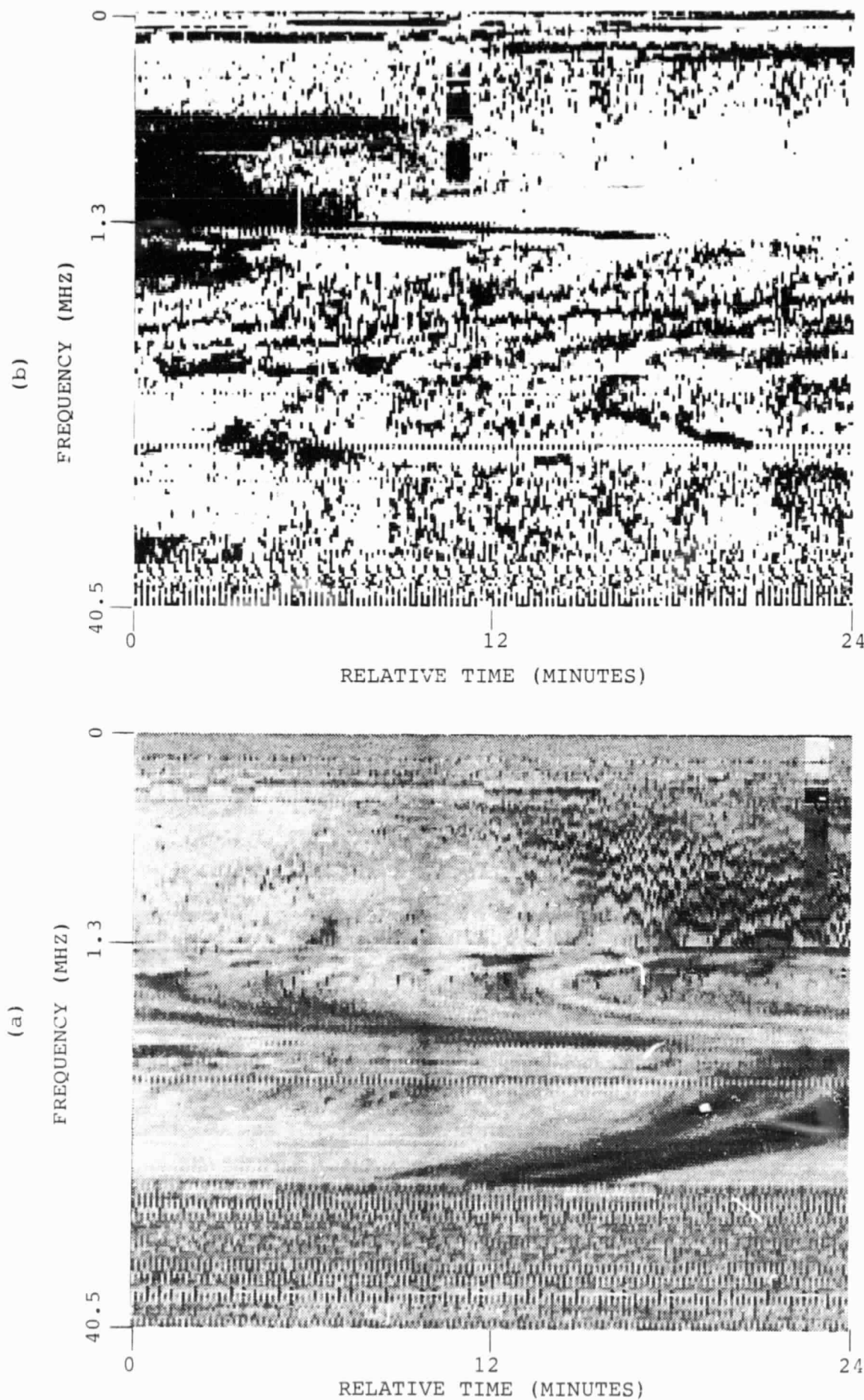
RELATIVE TIME (MINUTES)

Figure 1. 6-s PRA spectra. Frequency scales are piece-wise linear. a) Data from March 1 exhibiting MSA below 1.3 MHz and about 16 minutes after start of figure. b) Data from March 5 (day of encounter). Note MSA-like drifting emission bands.
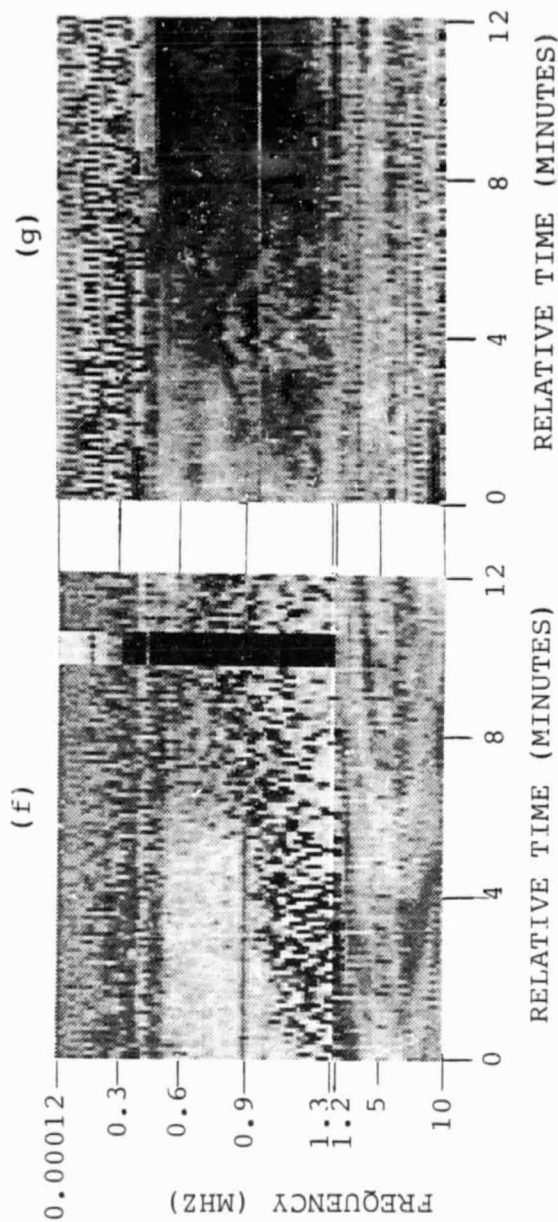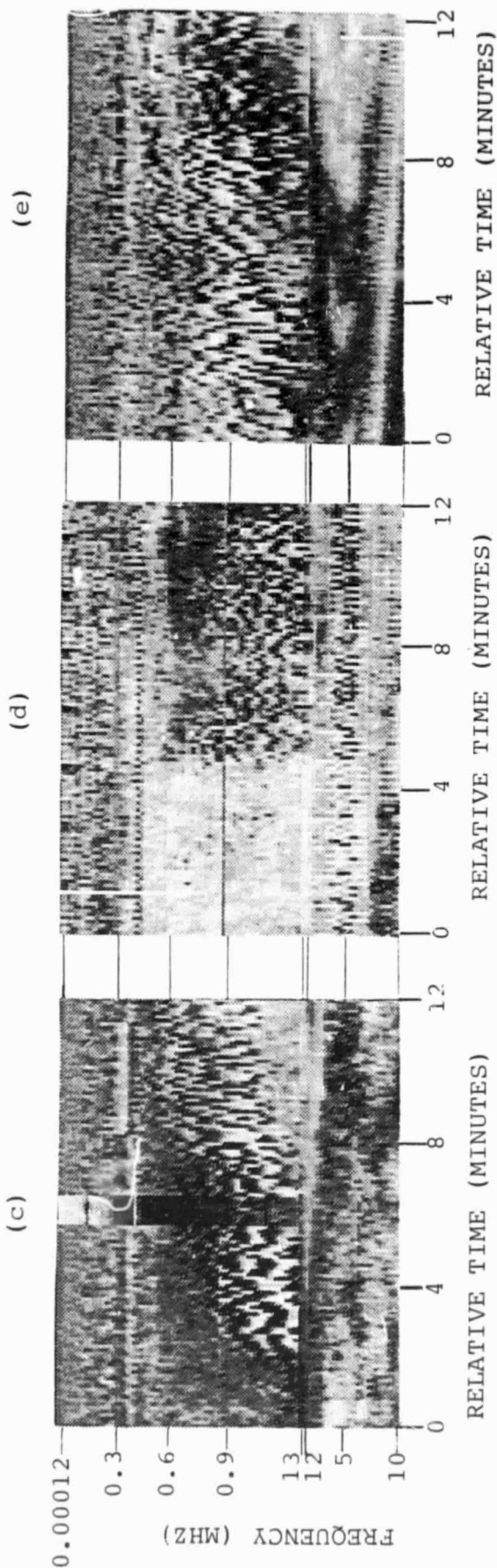
Figure 1 (continued). Examples of variation in MSA. Frequency scale is linear; starting times for a, b, c, d, e are $57^d13^h40^m$, $53^d11^h44^m$, $57^d8^h21^m$, $57^d15^h36^m$, and $53^d20^h57^m$, respectively.

The quoted uncertainties are estimated standard deviations based on the assumption that MSA possesses a Poisson-like distribution; MSA was observed too infrequently near encounter to reliably estimate the corresponding uncertainty. In fact, MSA was never observed during the ~13 hours of our observations made within 10 Jupiter radii (R-J) of the planet as reflected in the low near-encounter occurrence probability. This is probably the result of factors unique to encounter such as the range of spacecraft latitudes covered combined with low-frequency propagation effects near the Io plasma torus (IPT). We believe that the pre- and post- encounter probabilities are sufficiently close to the 12.6±1.2% over-all average occurrence probability to indicate that MSA experiences no significant local time effect. Similarly, the conditional probability of observing MSA during arc activity is 10.7±1.8%, close enough to the average MSA probability to indicate that observations of MSA and arcs are uncorrelated and, thus, that if the two emissions share the same source longitude, they must emerge at significantly different angles.

Periods thus far covered by our study appear as a function of CML and ϕIo (Io phase) in Figure 2 as lines which darken where MSA is observed. Clearly MSA is not strictly confined to specific regions of the CML-ϕIo plane as are, for example, high frequency S-bursts [Leblanc and Genova, 1981]. Nonetheless, there is a systematic variation of MSA occurrence with CML as indicated in Figure 3 which shows the MSA occurrence probability within each indicated 30 -wide CML range (error bars are single standard deviations estimated as above). MSA occurs more often at longitudes between 30 CML and 180 CML than at longitudes between 210 and 360 CML, behaving asymmetrically about the points where the north and south magnetic
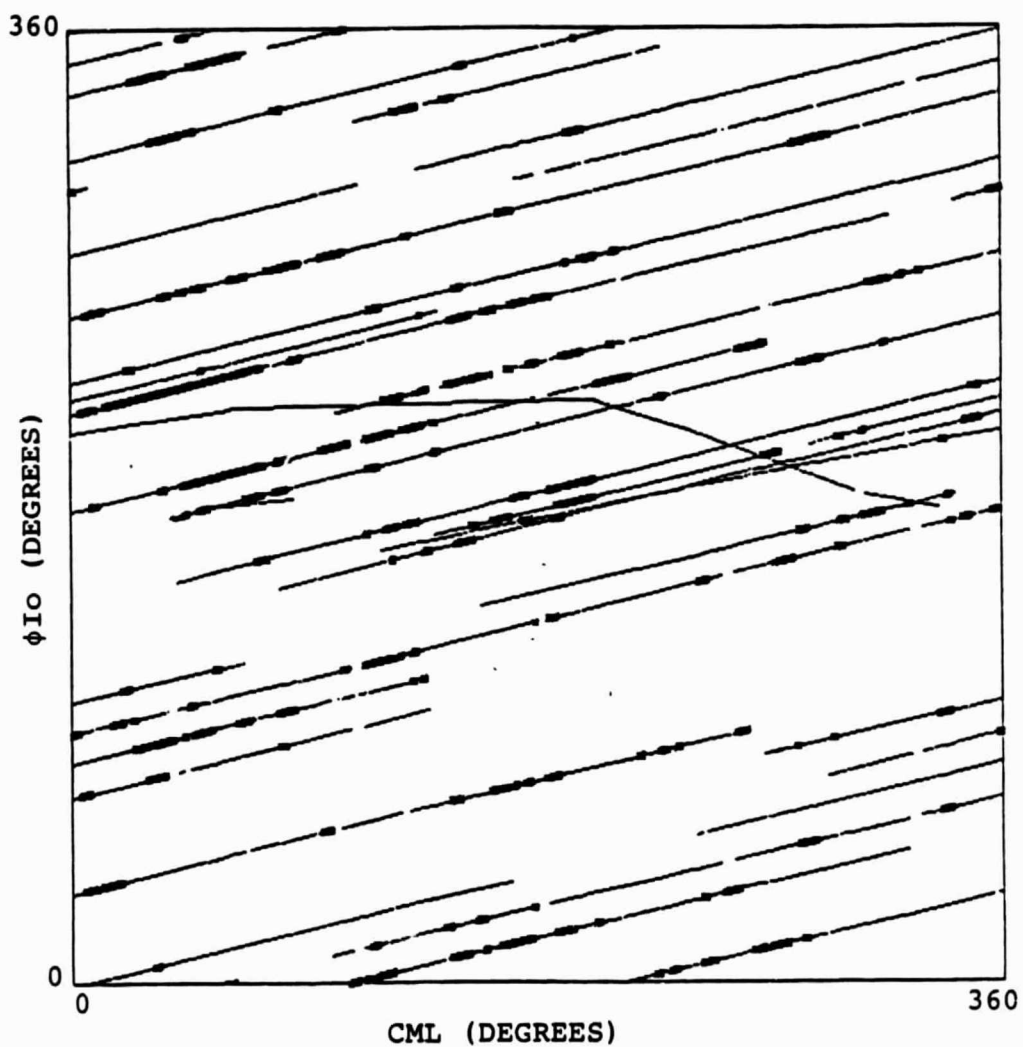
Figure 2. MSA occurrences in the CML-ϕIo plane. Lines
represent points covered by our study; thick
lines represent points where MSA was observed.
Note lack of confinement to specific regions
and variation in occurrence with CML.
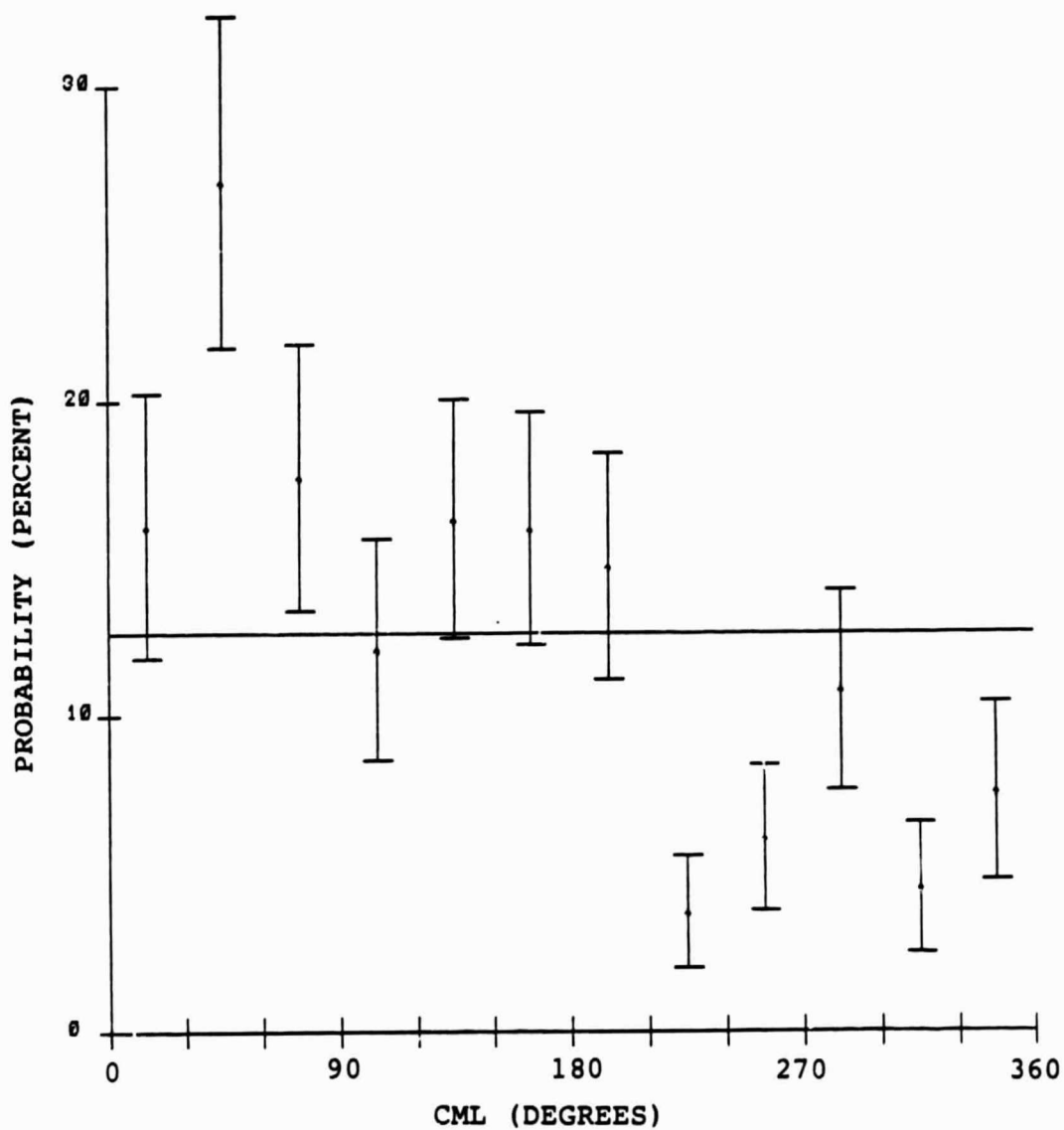
Figure 3.   MSA occurrence probability as a function of CML.
            Horizontal line represents the average MSA
            occurrence probability.   Note the asymmetric
            behavior about the magnetic pole crossings
            ($\sim$ 20 and $\sim$ 200 CML).

poles are maximally inclined toward the observer (~200 and ~20 CML, respectively). This is quite different from the behavior of other LF emissions which either show no long-term CML dependence (like nKOM, Boischot, et al. [1981]) or show symmetric behavior about the pole-crossings (like bKOM, Boischot, et al. [1981], or the bulk of HOM emission, Alexander, et al. [1981]). Asymmetries in the Jovian environment which may influence the occurrence of MSA include an O4 field strength at the foot of the L=6 shell which is weaker at all longitudes between 210 and 360 CML than at the highly MSA-active longitudes between 0 and 180 CML [Staelin, 1981], and a longitudinally variable IPT density which peaks in the low MSA activity region at ~250 CML [Pilcher and Morgan, 1980] or ~260 CML [Trafton, 1980], as determined from ground based observations of singly ionized sulfur.

Figure 4 shows a lack of variation in the occurrence probability of MSA with ϕIo. The data used in producing this figure, however, include the biased MSA-inactive near-encounter data, much of which was gathered at values of ϕIo slightly above 180. Figure 5 shows the variation of MSA occurrence probability with ϕIo when the near-encounter data are neglected. The increase in probability just beyond ϕIo=180 (the point where Io passes directly between Jupiter and the observer) is statistically significant and consistent with the hypothesis that currents emanating directly from Io stimulate MSA emission, suggesting a source region on or near the L=6 shell.

Work is beginning on the detailed study of single 6-s MSA spectra to gain insight into its source mechanism and on further consideration of MSA's time and frequency scales.
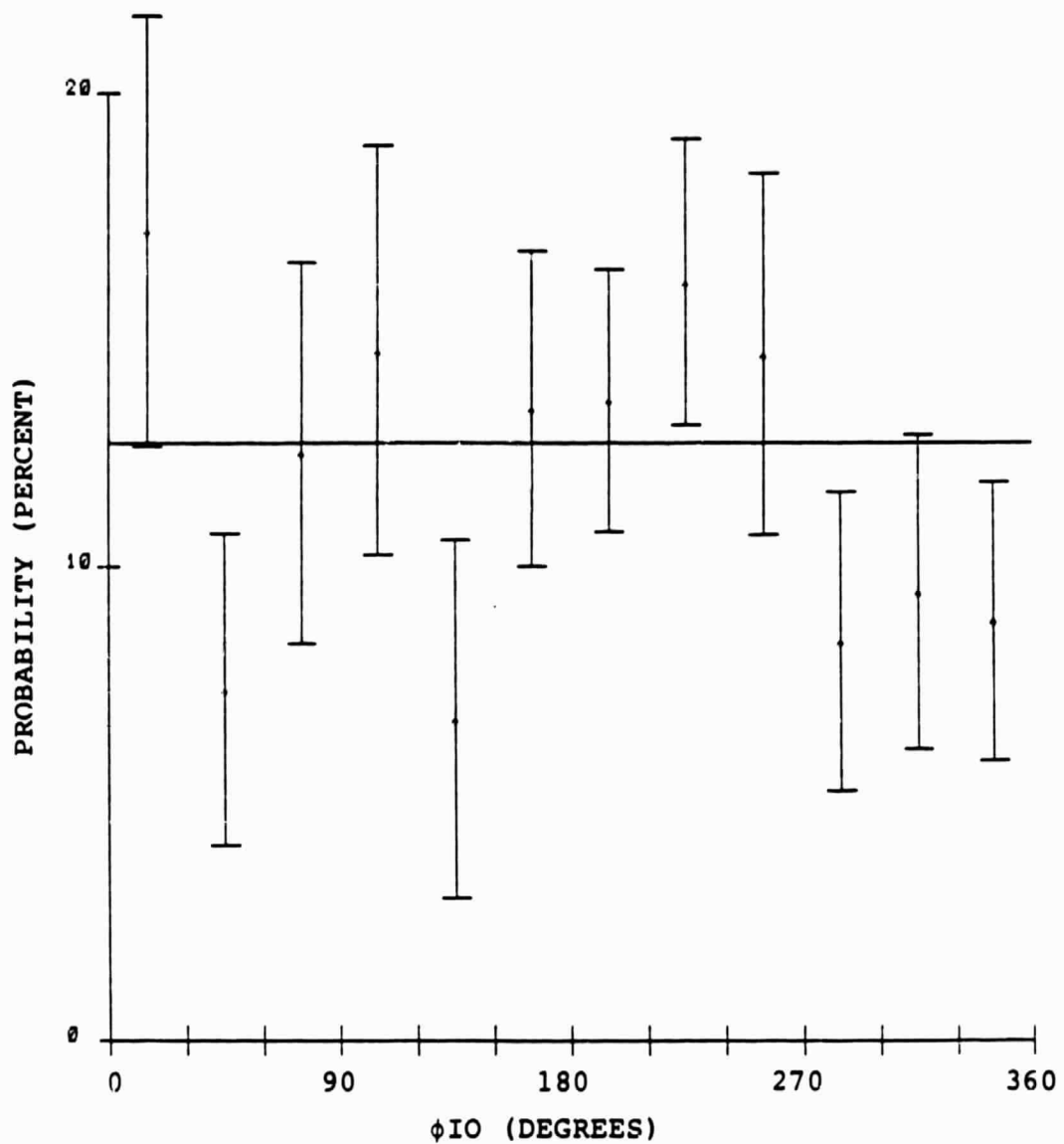
Figure 4. MSA occurrence probability as a function of ϕIo when near-encounter data are considered. Horizontal line represents the average MSA occurrence probability. Note the lack of systematic behavior.
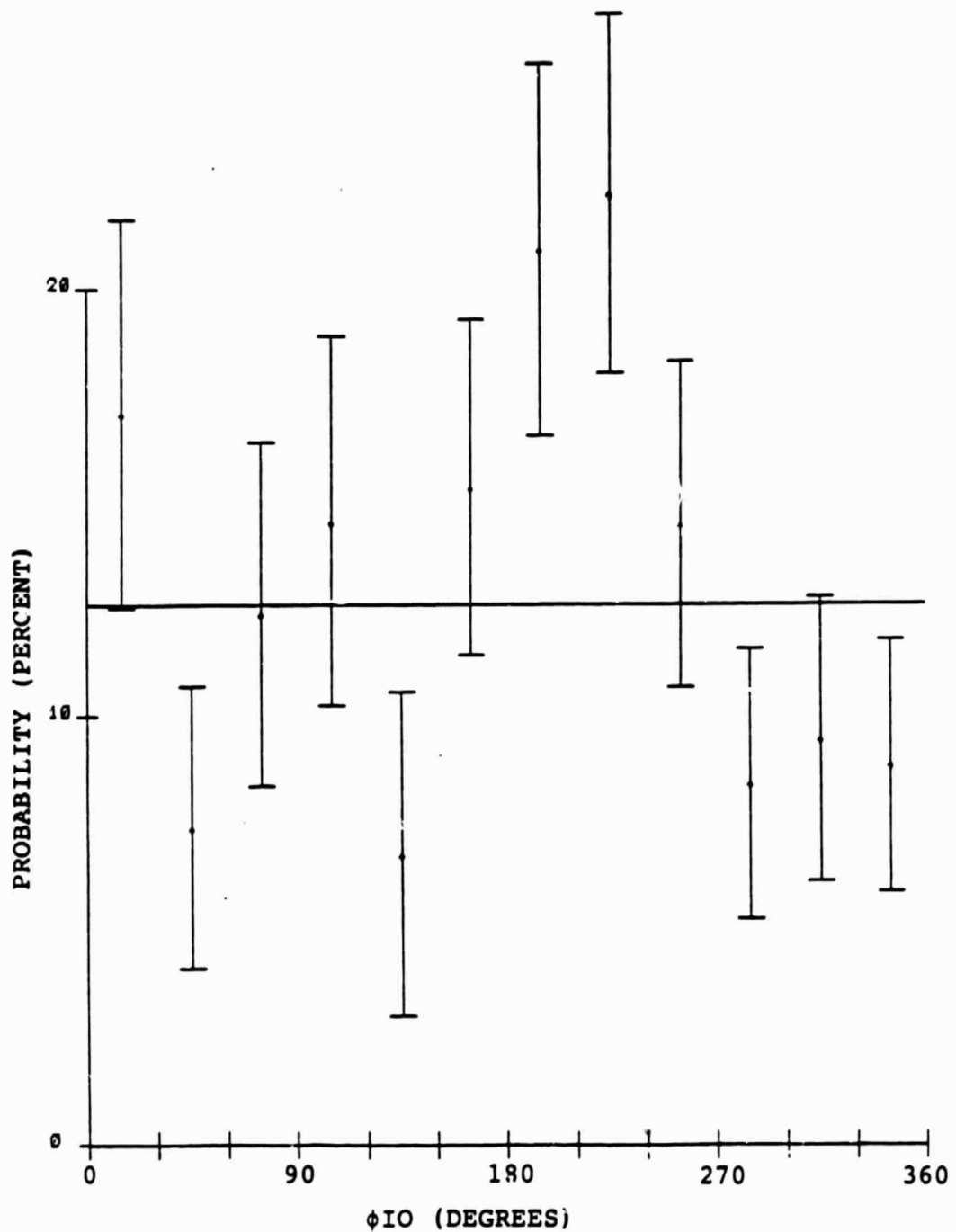
Figure 5. MSA occurrence probability as a function of φIo
when the near-encounter data are ignored.
Horizontal line represents the average MSA
occurrence probability. Note the sudden increase
in probability after φIo = 180.

Bibliography

Alexander, J. K., et al., "Synoptic Observations of Jupiter's Radio Emissions: Average Statistical Properties Observed by Voyager," Journ. Geophys. Res., 86, A10, 8529-8543 (1981).

Boischot, A., et al., "Radio Jupiter after Voyager: an overview of the Planetary Radio Astronomy observations," Journ. Geophys. Res., 86, A10, 8213-8226 (1981).

Leblanc, Y. and F. Genova, "The Jovian S Burst Sources," Journ. Geophys. Res., 86, A10, 8564-8568 (1981).

Pilcher, C. B., and J. S. Morgan, "The distribution of [SII] emission around Jupiter," Astrophys. J., 238, 375-380 (1980).

Staelin, D. H., "Character of the Jovian Decametric Arcs," Journ. Geophys. Res., 86, A10, 8581-8584 (1981).

Trafton, L., "Jovian SII Torus: Its Longitudinal Asymmetry," Icarus, 42, 111-124 (1980).